BAREKENG: Journal of Mathematics and Its Applications
June 2024 Volume 18 Issue 2 Page 1037–1052
P-ISSN: 1978-7227 E-ISSN: 2615-3017
https://doi.org/10.30598/barekengvol18iss2pp1037-1052

MATHEMATICAL MODEL OF REPELLENT EFFECT IN DENGUE TRANSMISSION

Dewi Handayani [1*], Audri Utami Gunadi[2], Ria Nurlita Rachmawati[3]

[1,2,3]*Industrial and Financial Mathematics Expertise Group,*
Faculty of Mathematics and Natural Sciences, Institut Teknologi Bandung
Jln Ganesa No.10, Bandung 40132, Indonesia

Corresponding author's e-mail: ***** ***dhandayanimtk@itb.ac.id***

Article History:

Received: 30th December 2023
Revised: 19th January 2024
Accepted: 21th March 2024
Published: 1st June 2024

Keywords:

Dengue;
Optimal Repellent Control;
Humans With Repellent;
Human Without Repellent;
Infected Mosquitos.

ABSTRACT

Dengue is a disease caused by the dengue virus, transmitted through the bite of an infected female Aedes aegypti. Dengue virus is a member of the genus Flavivirus, family Flaviviridae. Indonesia is one of the countries with the most dengue cases in Southeast Asia. Therefore, dengue transmission must be controlled to reduce the increase in dengue cases. One of the controls is by using repellents. Repellent is one of the human protection strategies to avoid mosquito bites used by spraying or smearing. This study models dengue transmission by reviewing the effect and control of repellent. A mathematical model of repellent effect and control in dengue transmission uses a SIR compartment model. The SIR model is modified by involving mosquitoes and the human population. Repellent is used in both susceptible humans, infected humans, and recovered humans. Numerical and analytical simulations are conducted to analyze the behavior of each compartment of the mosquito and human populations in dengue transmission. Analytical results show that the factors affecting the spread of infection are the transmission rate of the dengue virus and the loss of human-repellent protection. The transmission rate of dengue virus in the interval $[0.200, 0.550]$ *increases the infected human by 2.73%, while the rate of loss of human repellent protection in the interval* $[0.0001, 0.01]$ *increases the infected human by 0.03%. Optimal control is used to minimize the number of infected humans who do not use repellent. The results of numerical simulations on the optimal control problem show that an increase in the proportion of healthy humans who have campaign effect and use repellent regularly in the range of 14.67% can reduce infected individuals by 0.647%.*

How to cite this article:

D. Handayani, A. U. Gunadi and R. N. Rachmawati., "MATHEMATICAL MODEL OF REPELLENT EFFECT IN DENGUE TRANSMISSION," *BAREKENG: J. Math. & App.*, vol. 18, iss. 2, pp. 1037-1052, June, 2024.

Journal homepage: *https://ojs3.unpatti.ac.id/index.php/barekeng/*
Journal e-mail: *barekeng.math@yahoo.com; barekeng.journal@mail.unpatti.ac.id*

Research Article · Open Access

1. INTRODUCTION

Dengue is a dangerous disease caused by the dengue virus, which is transmitted through the bite of an infected female Aedes aegypti mosquito. The dengue virus has four serotypes, namely DEN-1, DEN-2, DEN-3, and DEN-4 [1]. Infection with one serotype will lead to the formation of antibodies against that specific serotype [2]. Aedes aegypti mosquitoes can become infected and act as vectors for dengue when they feed on the blood of individuals who are already infected with the virus [3]. After an incubation period of approximately 8 to 12 days, the mosquitoes can transmit the dengue virus to healthy individuals [4]. Generally, female Aedes aegypti mosquitoes bite two hours after sunrise and several hours before sunset [5]. The World Health Organization has stated that the recorded dengue cases have increased by over 8-fold in the past two decades [6]. The Ministry of Health of the Republic of Indonesia reported that Indonesia has shown an increasing trend in the cumulative number of dengue cases from January to September 2022, reaching 87.501 cases, including 816 fatalities. Among these cases, 38.96% occurred in the age group of 14 - 44 years, and 35.61% occurred in the age group of 5 - 14 years [7].

The transmission of dengue must be controlled to mitigate the increase in dengue cases. A study conducted by Prasetyo et al. (2020) [8] reviewed a disease spread model on dengue with control measures involving vaccination and repellent. However, vaccination has more impact for individuals previously been infected with dengue fever [9]. Therefore, a control model can be used to study how to reduce the spread and prevent the possible occurrence of Dengue epidemics. Repellents are chemical substances or household pesticides used to avoid insect bites or disturbances, and they can be applied through sprays or lotions, offering varying durations of protection depending on their types [10].

A mathematical model of the repellent effect in dengue transmission is constructed using the SIR compartments model. The SIR model is modified to include both mosquito population and the human population. Repellents are applied to humans, whether they are healthy, infected, or have recovered from the disease. Analytical solutions and numerical simulations are conducted to analyze the behavior of each compartment, both mosquito and human population, in the transmission of dengue.

2. RESEARCH METHODS

In this section, we present the model formulation, basic reproduction number, equilibrium points, stability, and the optimal control consisting of state, costate, and stationary conditions.

2.1 Model Formulation

A control problem of repellent effect in dengue transmission involving host and vector population is discussed here. The vector population is divided into two compartments, susceptible mosquitoes, $\boldsymbol{S_v}$, and infectious mosquitoes, $\boldsymbol{I_v}$. The human population is composed of susceptible humans without repellent $\boldsymbol{S_{hn}}$, susceptible humans with repellent $\boldsymbol{S_{hr}}$, infected humans without repellent $\boldsymbol{I_{hn}}$, infected humans with repellent $\boldsymbol{I_{hr}}$, recovered humans with repellent $\boldsymbol{R_{hn}}$ and recovered humans without repellent $\boldsymbol{R_{hr}}$. Transmission diagram between mosquitoes and humans are shown in Figure 1.

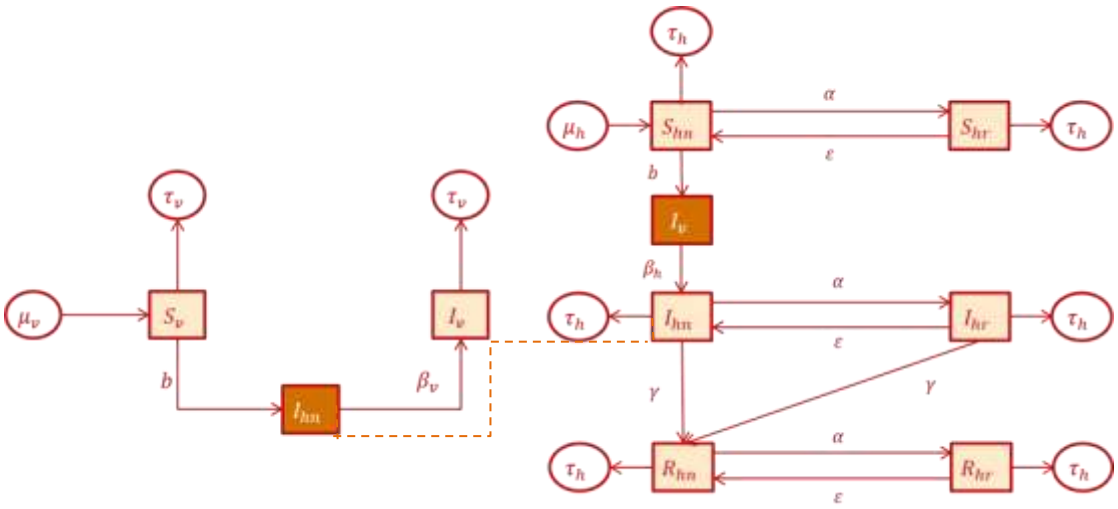

Figure 1. Compartment Diagram of the Dengue Transmission Model for Mosquito and Human Population

Let $\vec{X} = (\boldsymbol{S_v, I_v, S_{hn}, S_{hr}, I_{hn}, I_{hr}, R_{hn}, R_{hr}})^{\boldsymbol{T}}$, we consider the following dynamical system:

$$\frac{\boldsymbol{dS_v}}{\boldsymbol{dt}} = \boldsymbol{\mu_v N_v - \tau_v S_v - \frac{b\beta_v I_{hn} S_v}{N_h}} \quad (1)$$

$$\frac{\boldsymbol{dI_v}}{\boldsymbol{dt}} = \boldsymbol{\frac{b\beta_v I_{hn} S_v}{N_h} - \tau_v I_v} \quad (2)$$

$$\frac{dS_{hn}}{dt} = \mu_h N_h + \varepsilon S_{hr} - \tau_h S_{hn} - \alpha S_{hn} - \frac{b\beta_h I_v S_{hn}}{N_h} \quad (3)$$

$$\frac{dS_{hr}}{dt} = \alpha S_{hn} - \varepsilon S_{hr} - \tau_h S_{hr} \quad (4)$$

$$\frac{dI_{hn}}{dt} = \frac{b\beta_h I_v S_{hn}}{N_h} + \varepsilon I_{hr} - \tau_h I_{hn} - \alpha I_{hn} - \gamma I_{hn} \quad (5)$$

$$\frac{dI_{hr}}{dt} = \alpha I_{hn} - \varepsilon I_{hr} - \tau_h I_{hr} - \gamma I_{hr} \quad (6)$$

$$\frac{dR_{hn}}{dt} = \gamma(I_{hn} + I_{hr}) + \varepsilon R_{hr} - \tau_h R_{hn} - \alpha R_{hn} \quad (7)$$

$$\frac{dR_{hr}}{dt} = \alpha R_{hn} - \varepsilon R_{hr} - \tau_h R_{hr} \quad (8)$$

with $N_v = S_v + I_v$ the total of mosquito population and $N_h = S_{hn} + S_{hr} + I_{hn} + I_{hr} + R_{hn} + R_{hr}$ the total of human population. For the overall mosquito population, it holds that $\frac{dN_v}{dt} = (\mu_v - \tau_v)N_v$, and for all human population, it holds that $\frac{dN_h}{dt} = (\mu_h - \tau_h)N_h$. Assuming that N_v and N_h will be constant all the time, we get $\mu_v = \tau_v$ and $\mu_h = \tau_h$. Description and dimension for all compartments are showed in the **Table 1** and see **Table 2** for further detail about parameters value.

Table 1. Variables Description

Variable	Description	Dimension
S_v	Number of *Susceptible Mosquito*	Mosquito
I_v	Number of *Infected Mosquito*	Mosquito
S_{hn}	Number of *Susceptible Human without Repellent*	Human
S_{hr}	Number of *Susceptible Human with Repellent*	Human
I_{hn}	Number of *Infected Human without Repellent*	Human
I_{hr}	Number of *Infected Human with Repellent*	Human
R_{hn}	Number of *Recovered Human without Repellent*	Human
R_{hr}	Number of *Recovered Human with Repellent*	Human

Table 2. Parameters Description

Parameter	Description	Value	Unit	Reference
μ_v	Mosquito birth rate	0.03	Day^{-1}	[3]
τ_v	Mosquito death rate	0.03	Day^{-1}	[3]
b	Number of mosquito bites on humans every day	1	-	Assumed
β_v	Transmission rate of dengue virus from human to mosquito	0.375	Day^{-1}	[8]
μ_h	Average human birth rate	0.000042	Day^{-1}	[7, 8]
τ_h	Average human death rate	0.000042	Day^{-1}	[7, 8]
α	The rate of humans using repellent	0.01	Day^{-1}	[8]
ε	The rate of loss of repellent protection	0.001	Day^{-1}	Assumed
β_h	Transmission rate of dengue virus from mosquito to human	0.375	Day^{-1}	[3, 8]
γ	The rate of human recovery	0.3	Day^{-1}	[7]

Assuming that humans and mosquitoes are in equilibria, we could scale the human subpopulations by N_h and the mosquito subpopulations by N_v. The proportion of each individual can be expressed as:

$$s_v = \frac{S_v}{N_v}, i_v = \frac{I_v}{N_v}, s_{hn} = \frac{S_{hn}}{N_h}, s_{hr} = \frac{S_{hr}}{N_h}, i_{hn} = \frac{I_{hn}}{N_h}, i_{hr} = \frac{I_{hr}}{N_h}, r_{hn} = \frac{R_{hn}}{N_h}, r_{hr} = \frac{R_{hr}}{N_h}$$

By letting $\phi_S = \frac{S_v}{N_h}$ and $\phi_I = \frac{I_v}{N_h}$, we could obtain the normalized system of **Equation (1) - Equation (8)** is given by

$$\frac{ds_v}{dt} = \mu_v - \tau_v s_v - b\beta_v i_{hn}\phi_S \quad (9)$$

$$\frac{di_v}{dt} = b\beta_v i_{hn}\phi_S - \tau_v i_v \quad (10)$$

$$\frac{ds_{hn}}{dt} = \mu_h + \varepsilon s_{hr} - \tau_h s_{hn} - \alpha s_{hn} - b\beta_h \phi_I s_{hn} \quad (11)$$

$$\frac{ds_{hr}}{dt} = \alpha s_{hn} - \varepsilon s_{hr} - \tau_h s_{hr} \quad (12)$$

$$\frac{di_{hn}}{dt} = b\beta_h \phi_I s_{hn} + \varepsilon i_{hr} - \tau_h i_{hn} - \alpha i_{hn} - \gamma i_{hn} \quad (13)$$

$$\frac{di_{hr}}{dt} = \alpha i_{hn} - \varepsilon i_{hr} - \tau_h i_{hr} - \gamma i_{hr} \quad (14)$$

$$\frac{dr_{hn}}{dt} = \gamma(i_{hn} + i_{hr}) + \varepsilon r_{hr} - \tau_h r_{hn} - \alpha r_{hn} \quad (15)$$

$$\frac{dr_{hr}}{dt} = \alpha r_{hn} - \varepsilon r_{hr} - \tau_h r_{hr} \quad (16)$$

2.2 Basic Reproduction Ratio (R_0)

The basic reproduction ratio R_0 represents the expected number of secondary cases produced by a typical infected individual during its entire period of infectiousness in a completely susceptible population [11]. If $R_0 < 1$, the virus will not spread. If $R_0 > 1$, the virus will spread [12]. In this model, the value of R_0 is determined by defining the Next Generation Matrix [13] from the constructed compartments of the infected population

$$NGM_r = \begin{bmatrix} 0 & 0 & \frac{b\beta_h\mu_h\tau_v(\varepsilon+\tau_h)}{N_h\tau_h(\alpha+\varepsilon+\tau_h)} \\ 0 & 0 & 0 \\ \frac{b\beta_v\mu_v(\varepsilon+\gamma+\tau_h)}{N_h\tau_v[(\alpha+\gamma+\tau_h)(\varepsilon+\gamma+\tau_h)-\alpha\varepsilon]} & \frac{b\beta_v\mu_v\varepsilon}{N_h\tau_v[(\alpha+\gamma+\tau_h)(\varepsilon+\gamma+\tau_h)-\alpha\varepsilon]} & 0 \end{bmatrix}.$$

Furthermore, the largest eigenvalue of the NGM_r is the basic reproduction number with repellent

$$R_{0r} = \sqrt{\frac{b^2\beta_h\beta_v\mu_v(\varepsilon+\tau_h)(\varepsilon+\gamma+\tau_h)}{(\gamma+\tau_h)(\alpha+\varepsilon+\tau_h)(\alpha+\varepsilon+\gamma+\tau_h)}}. \quad (17)$$

R_{0r} is the basic reproduction ratio R_0, which is reviewed with the effect of repellent and is expressed as **Equation (17)**. This parameter R_{0r} can be used to estimate whether a new infection may end up in an epidemic and to estimate the severity of the epidemic when no treatment takes place.

2.3 Equilibrium Points

The equilibrium point is where the system stays stable, without any changes in subpopulation over time **[14]**. There are two types of the equilibriums, namely disease-free equilibrium and endemic equilibrium.

Disease-Free Equilibrium

This condition occurs when there is no infection **[15]**, so $i_{hn}(t) = i_{hr}(t) = i_v(t) = 0$. Then the **Equation (9) - Equation (16)** has a disease-free equilibrium

$$P_0 = \left(\frac{\mu_h(\varepsilon+\tau_h)}{\tau_h(\alpha+\varepsilon+\tau_h)}, \frac{\alpha\mu_h}{\tau_h(\alpha+\varepsilon+\tau_h)}, 0, 0, 0, 0, \frac{\mu_v}{\tau_v}, 0\right). \quad (18)$$

To analyze the stability of the disease-free equilibrium, the Jacobi matrix from the model, which is evaluated around the point P_0, is defined as

$$J_0 = \begin{bmatrix} -\alpha-\tau_h & \varepsilon & 0 & 0 & 0 & 0 & 0 & -\frac{b\beta_h\mu_h(\varepsilon+\tau_h)}{\tau_h(\alpha+\varepsilon+\tau_h)} \\ \alpha & -\varepsilon-\tau_h & 0 & 0 & 0 & 0 & 0 & \frac{b\beta_h\mu_h(\varepsilon+\tau_h)}{\tau_h(\alpha+\varepsilon+\tau_h)} \\ 0 & 0 & -\alpha-\gamma-\tau_h & \varepsilon & 0 & 0 & 0 & 0 \\ 0 & 0 & \alpha & -\varepsilon-\gamma-\tau_h & 0 & 0 & 0 & 0 \\ 0 & 0 & \gamma & \gamma & -\alpha-\tau_h & \varepsilon & 0 & 0 \\ 0 & 0 & 0 & 0 & \alpha & -\varepsilon-\tau_h & 0 & 0 \\ 0 & 0 & -\frac{b\beta_v\mu_v}{\tau_v} & 0 & 0 & 0 & -\tau_v & 0 \\ 0 & 0 & \frac{b\beta_v\mu_v}{\tau_v} & 0 & 0 & 0 & 0 & -\tau_v \end{bmatrix}. \quad (19)$$

The disease-free equilibrium point in **Equation (18)** will be locally asymptotically stable if all the real part of eigen values matrix in **Equation (19)** are negative and this condition is satisfied when

$$R_{0r} < \tau_v \text{ and } R_{0r} < \sqrt{\tau_v(\varepsilon+\gamma+\tau_h)\left(\frac{\tau_v}{(\alpha+\varepsilon+\gamma+\tau_h)} + \frac{(\alpha+\varepsilon+\gamma+\tau_h)}{(\gamma+\tau_h)}\right)}.$$

Endemic Equilibrium

This situation occurs when the infection spreads in population **[15]** so that $i_{hn}(t) \neq 0, i_{hr}(t) \neq 0$, and $i_v(t) \neq 0$. Let P_E is the endemic equilibrium point of model in **Equation (9) - Equation (16)**. Then, P_E can be expressed as:

$$P_E = \left(s_{hn}{}^E, s_{hr}{}^E, i_{hn}^E, i_{hr}^E, r_{hn}^E, r_{hr}^E, s_v^E, i_v^E\right) \quad (20)$$

where

$$s_{hn}^E = \frac{m_1(\varepsilon+\tau_h)}{w_1(\varepsilon+\gamma+\tau_h)}$$

$$s_{hr}^E = \frac{\alpha m_1}{w_1(\varepsilon+\gamma+\tau_h)}$$

$$i_{hn}^E = \frac{m_2}{w_1(\gamma+\tau_h)(\alpha+\varepsilon+\gamma+\tau_h)}$$

$$i_{hr}^E = \frac{\alpha m_2}{w_1(\gamma+\tau_h)(\varepsilon+\gamma+\tau_h)(\alpha+\varepsilon+\gamma+\tau_h)}$$

$$r_{hn}^E = \frac{\gamma m_2(\varepsilon+\tau_h)}{w_1\tau_h(\gamma+\tau_h)(\alpha+\varepsilon+\tau_h)(\varepsilon+\gamma+\tau_h)}$$

$$r_{hr}^E = \frac{m_2\alpha\gamma}{w_1\tau_h(\gamma+\tau_h)(\alpha+\varepsilon+\tau_h)(\varepsilon+\gamma+\tau_h)}$$

$$s_v^E = \frac{w_1(\gamma+\tau_h)(\alpha+\varepsilon+\gamma+\tau_h)}{b\beta_v w_2}$$

$$i_v^E = \frac{m_2}{\tau_v w_2}$$

and

$$m_1 = \tau_v(b\beta_v\mu_h(\varepsilon+\gamma+\tau_h)+\tau_v(\gamma+\tau_h)(\alpha+\varepsilon+\gamma+\tau_h))$$

$$m_2 = b^2\beta_h\beta_v\mu_h\mu_v(\varepsilon+\tau_h)(\varepsilon+\gamma+\tau_h)-\tau_h{\tau_v}^2(\gamma+\tau_h)(\alpha+\varepsilon+\tau_h)(\alpha+\varepsilon+\gamma+\tau_h)$$

$$w_1 = b\beta_v\big(b\beta_h\mu_v(\varepsilon+\tau_h)+\tau_h\tau_v(\alpha+\varepsilon+\tau_h)\big)$$

$$w_2 = b\beta_h(\varepsilon+\tau_h)\big(\beta_v\mu_h(\varepsilon+\gamma+\tau_h)+\tau_v(\alpha+\varepsilon+\gamma+\tau_h)\big).$$

To analyze the stability of the endemic equilibrium, the Jacobi matrix from the model, which is evaluated around the point P_E, is defined as:

$$J_e = \begin{bmatrix} -\frac{b\beta_h m_2}{\tau_v w_2}-\alpha-\tau_h & \varepsilon & 0 & 0 & 0 & 0 & 0 & -\frac{\tau_v w_2}{w_1(\varepsilon+\gamma+\tau_h)} \\ \alpha & -\varepsilon-\tau_h & 0 & 0 & 0 & 0 & 0 & \frac{\tau_v w_2}{w_1(\varepsilon+\gamma+\tau_h)} \\ \frac{b\beta_h m_2}{\tau_v w_2} & 0 & -\alpha-\gamma-\tau_h & \varepsilon & 0 & 0 & 0 & 0 \\ 0 & 0 & \alpha & -\varepsilon-\gamma-\tau_h & 0 & 0 & 0 & 0 \\ 0 & 0 & \gamma & \gamma & -\alpha-\tau_h & \varepsilon & 0 & 0 \\ 0 & 0 & 0 & 0 & \alpha & -\varepsilon-\tau_h & 0 & 0 \\ 0 & 0 & -\frac{\rho}{w_2} & 0 & 0 & 0 & -\frac{m_2}{\rho}-\tau_v & 0 \\ 0 & 0 & \frac{\rho}{w_2} & 0 & 0 & 0 & \frac{m_2}{\rho} & -\tau_v \end{bmatrix} \quad (21)$$

where $\rho = w_1(\gamma+\tau_h)(\alpha+\varepsilon+\gamma+\tau_h)$. The endemic equilibrium in **Equation (20)** will be locally asymptotically stable if all the real parts of eigen values matrix in **Equation (21)** are negative, and this condition is satisfied when

$$\sqrt{{\tau_v}^2-\frac{\tau_h}{(\gamma+\tau_h)(\alpha+\varepsilon+\gamma+\tau_h)}} < R_{0r} < \sqrt{{\tau_v}^2-\frac{(\varepsilon+\tau_h)(\alpha+\varepsilon+2\tau_h)}{(\gamma+\tau_h)(\alpha+\varepsilon+\tau_h)(\alpha+\varepsilon+\gamma+\tau_h)}}.$$

2.4 Optimal Control

Given the disease model **Equation (9-16)**, we want to design the repellent treatment rate u_1 for the human population and the proportion of providing a campaign u_2 about the importance of mosquito repellent for susceptible humans s_{hn}, such that we minimize the number of infected humans without repellent i_{hn}. Assuming that healthy humans who receive the campaign immediately become aware of the need to use mosquito repellent regularly, this population is classified as a recovered population.

Let $\vec{x} = (s_v,\ i_v,\ s_{hn},\ s_{hr},\ i_{hn},\ i_{hr},\ r_{hn},\ r_{hr})^T$ and the dynamical model with repellent control is expressed as $\dot{\vec{x}} = \left(f_1(\vec{x}), f_2(\vec{x}), f_3(\vec{x}), f_4(\vec{x}), f_5(\vec{x}), f_6(\vec{x}), f_7(\vec{x}), f_8(\vec{x})\right)^T$ and defined as :

$$\frac{ds_v}{dt} = f_1(\vec{x}) = \mu_v - \tau_v s_v - b\beta_v i_{hn}\frac{s_v N_v}{N_h} \tag{22}$$

$$\frac{di_v}{dt} = f_2(\vec{x}) = b\beta_v i_{hn}\frac{s_v N_v}{N_h} - \tau_v i_v \tag{23}$$

$$\frac{ds_{hn}}{dt} = f_3(\vec{x}) = \mu_h(1-u_2) + \varepsilon s_{hr} - \tau_h s_{hn} - \alpha s_{hn}u_1 - b\beta_h s_{hn}\frac{i_v N_v}{N_h} \tag{24}$$

$$\frac{ds_{hr}}{dt} = f_4(\vec{x}) = \alpha s_{hn}u_1 - \varepsilon s_{hr} - \tau_h s_{hr} \tag{25}$$

$$\frac{di_{hn}}{dt} = f_5(\vec{x}) = b\beta_h s_{hn}\frac{i_v N_v}{N_h} + \varepsilon i_{hr} - \tau_h i_{hn} - \alpha i_{hn}u_1 - \gamma i_{hn} \tag{26}$$

$$\frac{di_{hr}}{dt} = f_6(\vec{x}) = \alpha i_{hn}u_1 - \varepsilon i_{hr} - \tau_h i_{hr} - \gamma i_{hr} \tag{27}$$

$$\frac{dr_{hn}}{dt} = f_7(\vec{x}) = \gamma(i_{hn} + i_{hr}) + \varepsilon r_{hr} - \tau_h r_{hn} - \alpha r_{hn}u_1 \tag{28}$$

$$\frac{dr_{hr}}{dt} = f_8(\vec{x}) = \alpha r_{hn}u_1 + \mu_h u_2 - \varepsilon r_{hr} - \tau_h r_{hr} \tag{29}$$

To find a suitable compromise between the minimal number of infected individuals and the costs of the campaign, we consider the following cost-functional

$$J(u_1, u_2) = \min_{u_1, u_2} \int_0^{t_{end}} [Ai_{hn} + B{u_1}^2 + C{u_2}^2]\, dt \tag{30}$$

where feasible control input set is written as $\vec{u} = \{(u_1, u_2): 0 \le u_1 \le 1 \text{ and } 0 \le u_2 \le 1\}$. The weighting parameter A is used for the state variables $\vec{x}$ in **Equation (22) - Equation (29)** and the weighting parameters B and C are used for the control variables $\vec{u} = (u_1, u_2)$. Since we are mainly interested in minimizing the number of the infected human i_{hn}, we set $A > 0$. On the other hand, we want to minimize the costs of repellent and campaign. The costs of the treatment use are more-or-less proportional to the repellent rates hence we also choose $B, C > 0$ as usual. According to **Equation (30)** and $\vec{\lambda} = (\lambda_1, \lambda_2, \lambda_3, \lambda_4, \lambda_5, \lambda_6, \lambda_7, \lambda_8)^T$ as costate or adjoint variables, we define the Hamiltonian function as:

$$H(\vec{x}, \vec{u}, \vec{\lambda}, t) = Ai_{hn} + B{u_1}^2 + C{u_2}^2 + \vec{\lambda}\,\dot{\vec{x}}$$

Proposition 1. Consider $\vec{x} = (s_v,\ i_v,\ s_{hn},\ s_{hr},\ i_{hn},\ i_{hr},\ r_{hn},\ r_{hr})^T$ as state variables and $\vec{u} = (u_1,\ u_2)^T$ as control variables. If the objective function is defined as in **Equation (30)**, then the optimal control solution must exist, such that $J({u_1}^*, {u_2}^*) = \min J(u_1, u_2)$.

Proof. Optimal control solution exists if these four conditions hold:

1. The state variables and the corresponding control variables are non-empty sets.
2. Suppose that $\Gamma = \{(u_1,\ u_2) \mid 0 \le u_1 \le {u_1}^{max}, 0 \le u_2 \le {u_2}^{max}\}$. Hence, Γ is closed and convex.
3. The model **Equation (22-29)** are nonlinear and depend on the control variables.
4. Suppose that the objective function of system is defined as follows

$$J(u) = \int_{t_0}^{T} L(x(t), u(t), t)\, dt = \int_0^{t_{end}} [Ai_{hn} + B{u_1}^2 + C{u_2}^2]\, dt$$

with $[t_0, T]$ is a time interval and $L(x(t), u(t), t)$ is a weight function that depends on the state and the input at time interval $[t_0, T]$. Then, there are nonnegative constants l_1, l_2 and $n > 1$ so that the weight function $L(x(t), u(t), t)$ is convex and satisfies

$$L(x(t), u(t), t) \ge l_1 + l_2(|u_1|^2 + |u_2|^2)^{\frac{n}{2}}.$$

Condition 1 is satisfied since the state and control variables are nonempty and finite with $s_v, s_{hn}, s_{hr} > 0$, $i_v, i_{hn}, i_{hr}, r_{hn}, r_{hr} \geq 0$, $0 \leq u_1 \leq 1$, and $0 \leq u_2 \leq 1$. Condition 2 is satisfied by the definition of Γ. From Condition 1, $u_1^{max} = u_2^{max} = 1$ and we can get $\Gamma = \{(u_1,\ u_2) \mid 0 \leq u_1 \leq 1, 0 \leq u_2 \leq 1\}$. Condition 3 is clearly satisfied, and the system in **Equation (22) - Equation (29)** depends on the control variables $\vec{u}$. It will be shown that Condition 4 is satisfied. Note that, L is clearly convex and depends on the control variables $\vec{u}$. We have to choose nonnegative constants l_1 and l_2. Suppose that $l_1 = \min Ai_{hn} \leq Ai_{hn}$, with $i_{hn} > 0$ and $l_2 = \min(B, C)$ with $B, C > l_2$. With $n = 2 > 1$, we can get

$$L(x(t), u(t), t) = Ai_{hn} + B{u_1}^2 + C{u_2}^2 \geq l_1 + l_2(|u_1|^2 + |u_2|^2)^{\frac{n}{2}}$$

Consequently, L is finite and Condition 4 is satisfied. The optimal control solution $u^*(t)$ must be exist. ∎

Proposition 2. If $(\vec{x}^*(t), \vec{u}^*(t))$ is the optimal control solution with $\vec{x}^* = (s_v^*, i_v^*, s_{hn}^*, s_{hr}^*, i_{hn}^*, i_{hr}^*, r_{hn}^*, r_{hr}^*)^T$ and $\vec{u}^* = (u_1^*, u_2^*)^T$, then there is adjoint variable $\vec{\lambda}^*(t)$ that satisfies the costate equations $\dot{\vec{\lambda}} = -\frac{\partial H}{\partial \vec{x}}$ with $\vec{\lambda} = (\lambda_1, \lambda_2, \lambda_3, \lambda_4, \lambda_5, \lambda_6, \lambda_7, \lambda_8)^T$ and expressed as :

$$\dot{\lambda_1} = -\frac{\partial H}{\partial s_v} = \lambda_1\left(\tau_v + b\beta_v i_{hn}\frac{N_v}{N_h}\right) - \lambda_2 b\beta_v i_{hn}\frac{N_v}{N_h} \tag{31}$$

$$\dot{\lambda_2} = -\frac{\partial H}{\partial i_v} = \lambda_2\tau_v + \lambda_3 b\beta_h s_{hn}\frac{N_v}{N_h} - \lambda_5 b\beta_h s_{hn}\frac{N_v}{N_h} \tag{32}$$

$$\dot{\lambda_3} = -\frac{\partial H}{\partial s_{hn}} = \lambda_3\left[\tau_h s_{hn} + \alpha u_1 - b\beta_h\frac{i_v N_v}{N_h}\right] - \lambda_4\alpha u_1 - \lambda_5 b\beta_h\frac{i_v N_v}{N_h} \tag{33}$$

$$\dot{\lambda_4} = -\frac{\partial H}{\partial s_{hr}} = -\lambda_3\varepsilon + \lambda_4[\varepsilon + \tau_h] \tag{34}$$

$$\dot{\lambda_5} = -\frac{\partial H}{\partial i_{hn}} = \lambda_1 b\beta_v\frac{s_v N_v}{N_h} - \lambda_2 b\beta_v\frac{s_v N_v}{N_h} + \lambda_5[\tau_h + \alpha u_1 + \gamma] - \lambda_6\alpha i_{hn}u_1 - \lambda_7\gamma - A \tag{35}$$

$$\dot{\lambda_6} = -\frac{\partial H}{\partial i_{hr}} = -\lambda_5\varepsilon + \lambda_6[\varepsilon + \tau_h + \gamma] - \lambda_7\gamma \tag{36}$$

$$\dot{\lambda_7} = -\frac{\partial H}{\partial r_{hn}} = \lambda_7[\tau_h + \alpha u_1] - \lambda_8\alpha u_1 \tag{37}$$

$$\dot{\lambda_8} = -\frac{\partial H}{\partial r_{hr}} = -\lambda_7\varepsilon + \lambda_8[\varepsilon + \tau_h] \tag{38}$$

with $\vec{\lambda}(T) = 0$ and the stationary the conditions $\frac{\partial H}{\partial \vec{u}} = 0$ satisfies

$$2Bu_1^* + s_{hn}^*(\lambda_4 - \lambda_3) + i_{hn}^*(\lambda_6 - \lambda_5) + r_{hn}^*(\lambda_8 - \lambda_7) = 0$$

$$2Cu_2^* - \lambda_3\mu_h + \lambda_8\mu_h = 0.$$

Then, we can obtain the optimal control solution

$$u_1^* = \max\left\{\min\left\{\frac{\alpha[s_{hn}^*(\lambda_3 - \lambda_4) + i_{hn}^*(\lambda_5 - \lambda_6) + r_{hn}^*(\lambda_7 - \lambda_8)]}{2B}, 1\right\}, 0\right\}, \tag{39}$$

$$u_2^* = \max\left\{\min\left\{\frac{(\lambda_3 - \lambda_8)\mu_h}{2C}, 1\right\}, 0\right\}. \tag{40}$$

Proof. Note that the Hamiltonian function is used to determine $\vec{\lambda}^*(t)$ that satisfies **Equation (31-38)** by considering $\vec{x}(t) = \vec{x}^*(t)$, then the Hamiltonian function is differentiated against $\vec{x}$. Afterward, the optimal control $\vec{u}^*$is obtained from these following steps:

First, substitute the values of u_1^* and u_2^* in **Equation (39) - Equation (40)** to the system in **Equation (22) - Equation (29)**. Thus, a new Hamiltonian function H^* at $(\vec{x}^*, \vec{u}^*, \vec{\lambda}, t)$ is obtained as follows

$$H^* = Ai_{hn}^* + B\left(\max\left\{\min\left\{\frac{\alpha[s_{hn}^*(\lambda_3-\lambda_4)+i_{hn}^*(\lambda_5-\lambda_6)+r_{hn}^*(\lambda_7-\lambda_8)]}{2B},1\right\},0\right\}\right)^2 + C\left(\max\left\{\min\left\{\frac{(\lambda_3-\lambda_8)\mu_h}{2C},1\right\},0\right\}\right)^2 + \lambda_1\frac{ds_v^*}{dt} + \lambda_2\frac{di_v^*}{dt} + \lambda_3\frac{ds_{hn}^*}{dt} + \lambda_4\frac{ds_{hr}^*}{dt} + \lambda_5\frac{di_{hn}^*}{dt} + \lambda_6\frac{di_{hr}^*}{dt} + \lambda_7\frac{dr_{hn}^*}{dt} + \lambda_8\frac{dr_{hr}^*}{dt}.$$

3. RESULTS AND DISCUSSION

In this model, the endemic status of the disease depends on the transmission toward incoming viruses to the individual from mosquito bites. The larger the invasion rate β_h and the loss of repellent protection ϵ, the chance is higher to catch the disease. On the contrary, with the increase in the rate of using repellent for human populations, the risk of infection is lower. Based on the model in **Equation (9)** - **Equation (16)** with parameter values from **Table 2** and initial values of $s_{hn} = 0.60, s_{hr} = 0.30, i_{hn} = 0.06, i_{hr} = 0.03, s_v = 0.67$, and $i_v = 0.33$, the variation for α, β_h and ϵ shows in **Figure 2**, **Figure 3** and **Figure 4**.

The variation of the parameter will measure how sensitive or influential the parameter is in the spread of the disease for dynamics of s_{hn} and i_{hn}. **Figure 2** the dynamics of s_{hn} and i_{hn} for different rate of using repellent, α. An increase in α leads to a decline in the dynamic of s_{hn}. The behavior of i_{hn} increases until maximum value and after the peak of infection occurs, i_{hn} will decrease more significantly as α increases.

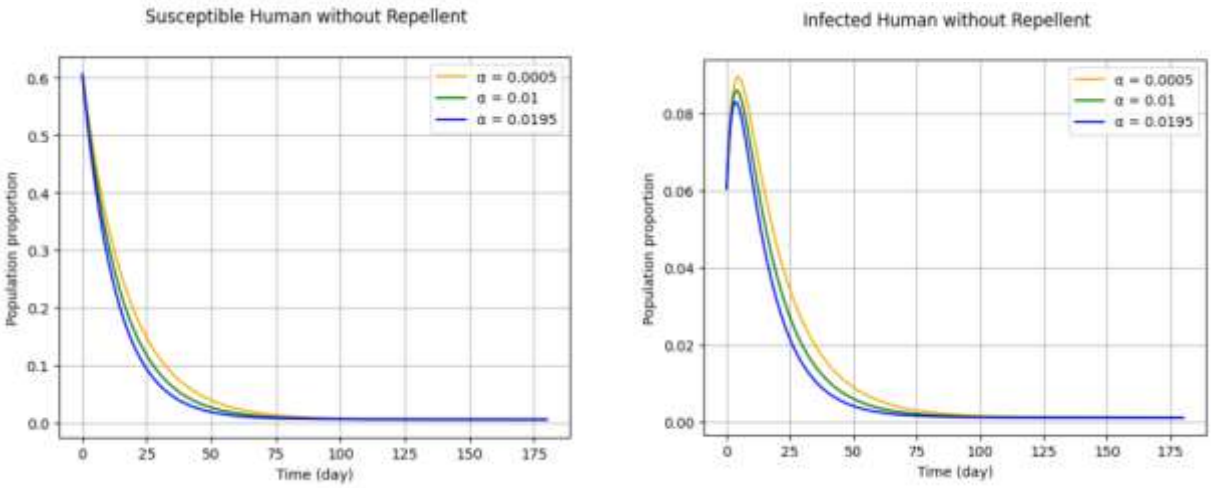

(a) **(b)**

Figure 2. Variations in The Rate of Humans Using Repellent
(a) Susceptible Human without Repellent, (b) Infected Human without Repellent

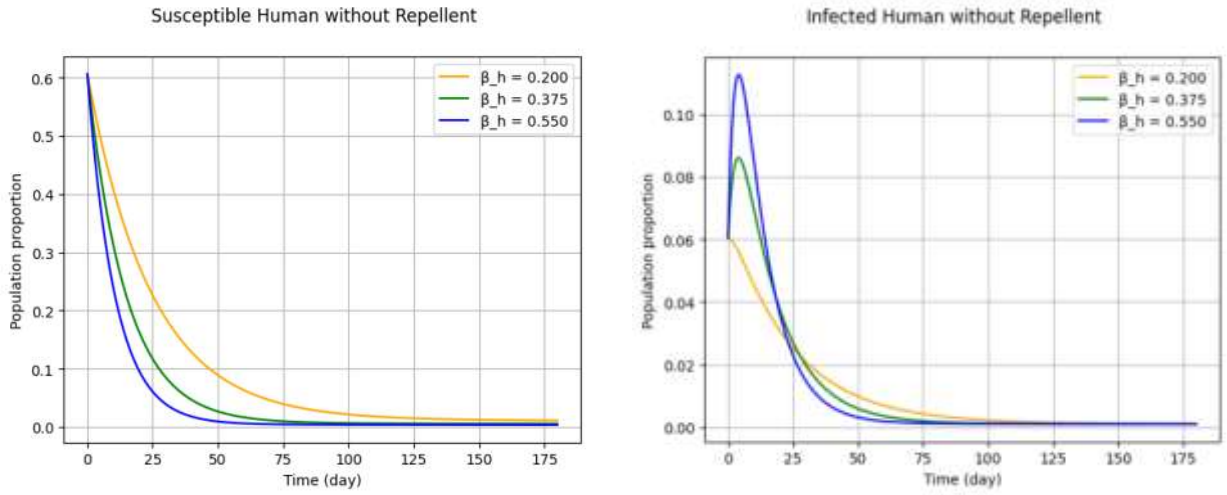

(a) **(b)**

Figure 3. Variations in The Transmission Rate of Dengue Virus
(a) Susceptible Human without Repellent, (b) Infected Human without Repellent

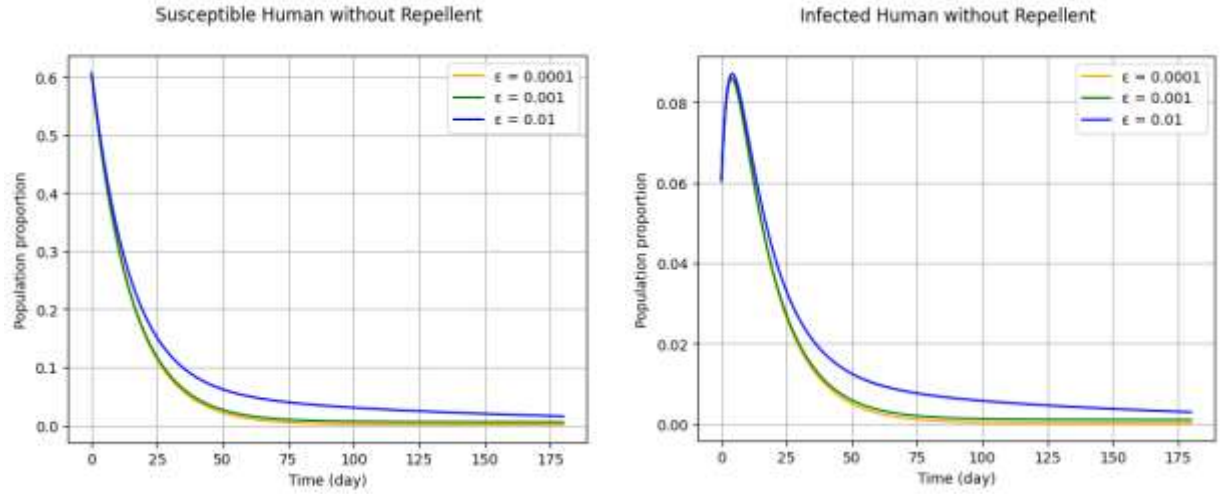

(a) **(b)**

Figure 4. Variations in The Rate of Loss of Repellent Protection
(a) Susceptible Human without Repellent, (b) Infected Human without Repellent

Figure 3 shows the dynamics of s_{hn} and i_{hn} for different contact rate between susceptible human without repellent with infected mosquitos, β_h. An increase of β_h will decrease s_{hn} more rapidly. For high value of β_h, there is a high value of i_{hn} in early, but it also will decrease i_{hn} more rapidly. The rate of loss of repellent protection, ϵ, represents the duration for which repellents provide protection against mosquito bites. A lower rate implies an extended period of effectiveness. As observed in **Figure 4**, a longer duration of repellent protection leads to increase s_{hn} and i_{hn}.

Numerical simulations of the optimal control problem are carried out for two scenarios, namely, the case of prevention to control the campaign rate for healthy humans and the case of epidemic reduction to control the usage rate of repellent. The case of prevention occurs at the early state of transmission, i.e., when the number of infected people is still relatively small before the start of the repellent treatment. In the case of epidemic reduction, the repellent treatment starts during the outbreak period, i.e., when the number of infected people is significantly large. As an initial condition, we assume that in the field, the ratio between the mosquito and human population is almost the same. With this ratio, the corresponding basic reproductive ratio is about 1.44 before the start of the repellent treatment. This condition leads the population to endemic equilibrium.

Figure 5 - **Figure 7** shows the results for controlling repellent treatment rate (u_1) for human populations. **Figure 5** shows the dynamic of s_{hn} and s_{hr} with and without control u_1. From **Figure 5**(a), s_{hn} with control decreases slower by 1.425% than without control. While in **Figure 5**(b), s_{hr} with control

decreases to 6.066% compared to without control. Therefore, with control of repellent treatment rate (u_1), the potential for transmission in healthy human populations will tend to have a small chance.

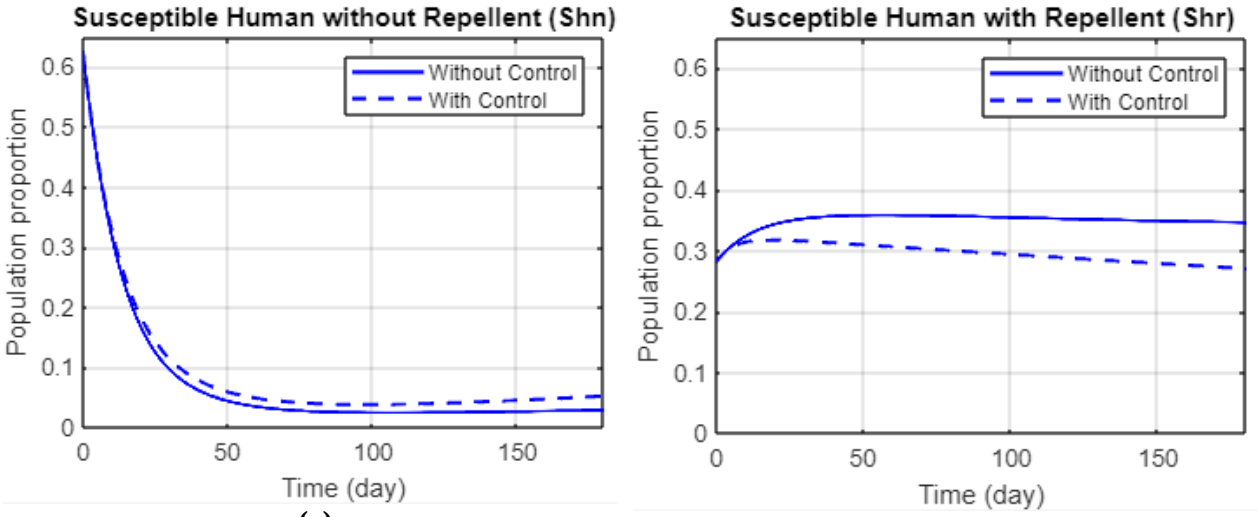

(a) **(b)**

Figure 5. Numerical Simulation Result of Controlling the Usage Rate of Repellent (a) Susceptible Human without Repellent, (b) Susceptible Human with Repellent

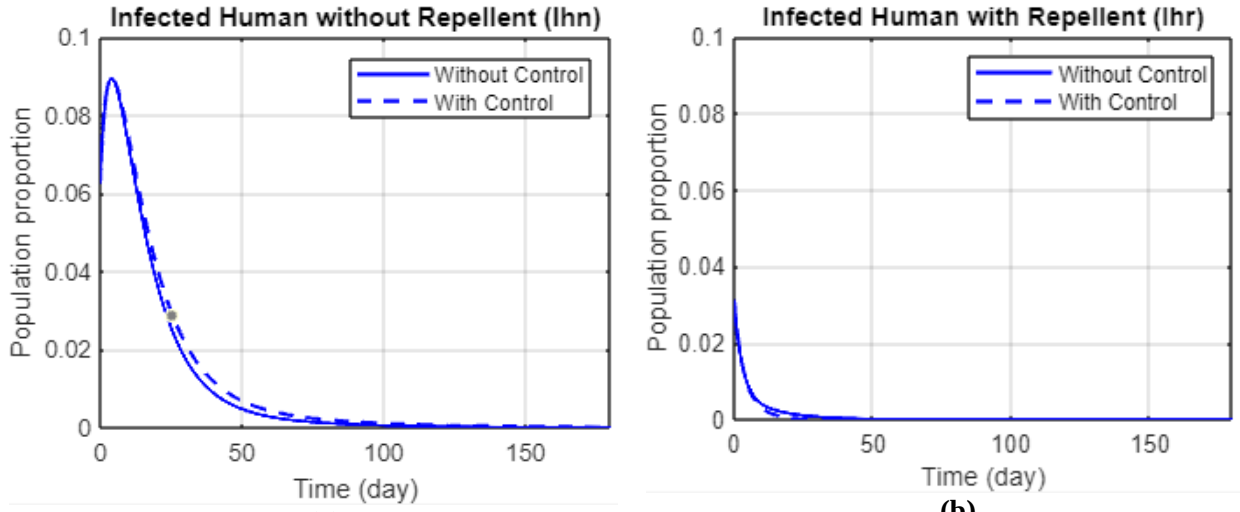

(a) **(b)**

Figure 6. Numerical Simulation Result of Controlling the Usage Rate of Repellent (a) Infected Human without Repellent, (b) Infected Human with Repellent

Figure 6 shows the dynamic of i_{hn} and i_{hr} with and without control u_1. **Figure 6**(a) shows that after the peak of infection, i_{hn} without control decreases faster by about 0.443% than the i_{hn} with control. Meanwhile, **Figure 6**(b) shows i_{hr} with control decreases to 0.146% compared to the i_{hr} without control. **Figure 7** shows the dynamic of r_{hn} and r_{hr} with and without control u_1. From **Figure 7**(a), r_{hn} with control increases to 23.965% compared to the r_{hn} without control. Meanwhile, **Figure 7**(b) shows r_{hr} with control decreases to 19.420% from r_{hr} without control and as time goes by, the decrease will be even greater. Therefore, control of repellent treatment rate (u_1) can work effectively to minimize the infected population and to maximize the recovered population.

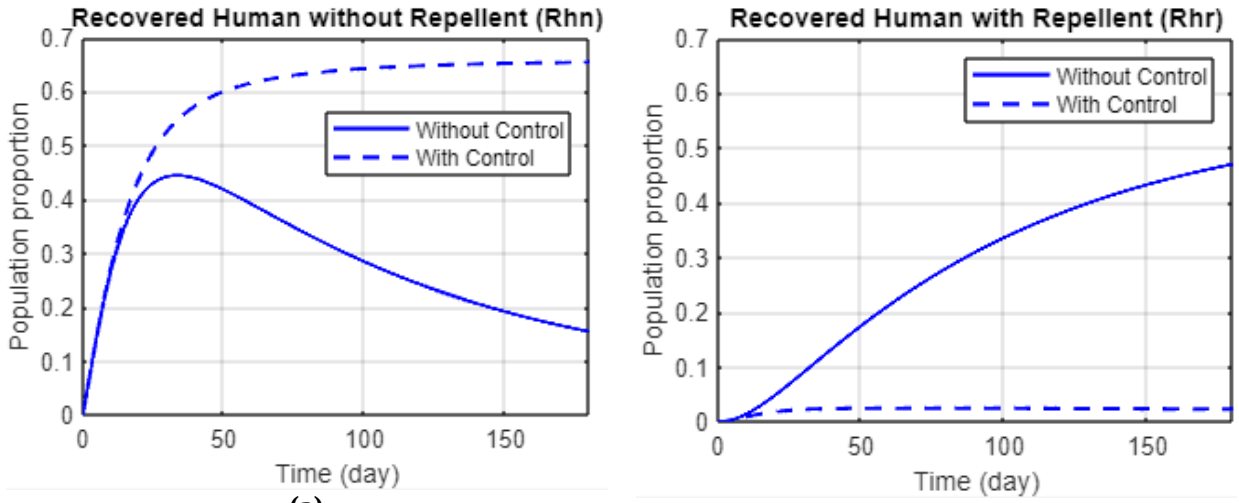

(a) **(b)**

Figure 7. Numerical Simulation Result of Controlling the Usage Rate of Repellent (a) Recovered Human without Repellent, (b) Recovered Human with Repellent

Figure 8 - **Figure 10** shows the dynamics for human population if the control campaign applied and implies the repellent used regularly (u_2) since early of infection period. **Figure 8** shows the dynamic of s_{hn} and s_{hr} without and with control u_2. From **Figure 8**(a), s_{hn} with control increases slower by 2.613% than s_{hn} without control. And **Figure 8**(b) shows that s_{hr} with control decreases quite large by 9.381% compared to the s_{hr} without control. As a result, the successful campaign to use repellent in the early infection period is effective in reducing the potential for transmission. Therefore, the number of healthy humans who use repellents will increase.

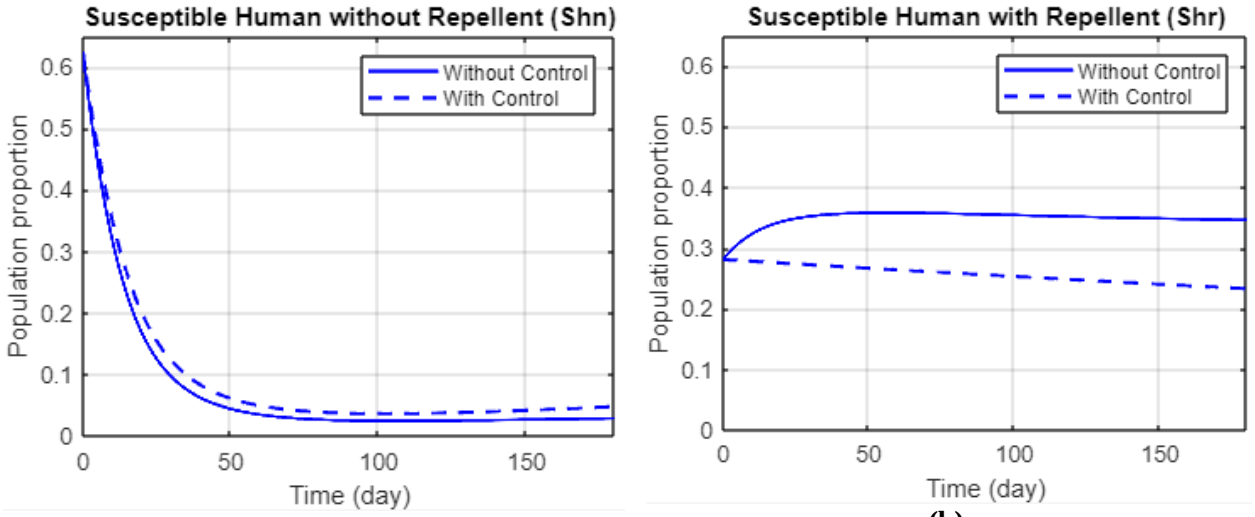

(a) **(b)**

Figure 8. Numerical Simulation Result of Controlling the Proportion Healthy Humans Who Have Impacted by Campaign and Used Repellent Regularly (a) Susceptible Human without Repellent, (b) Susceptible Human with Repellent

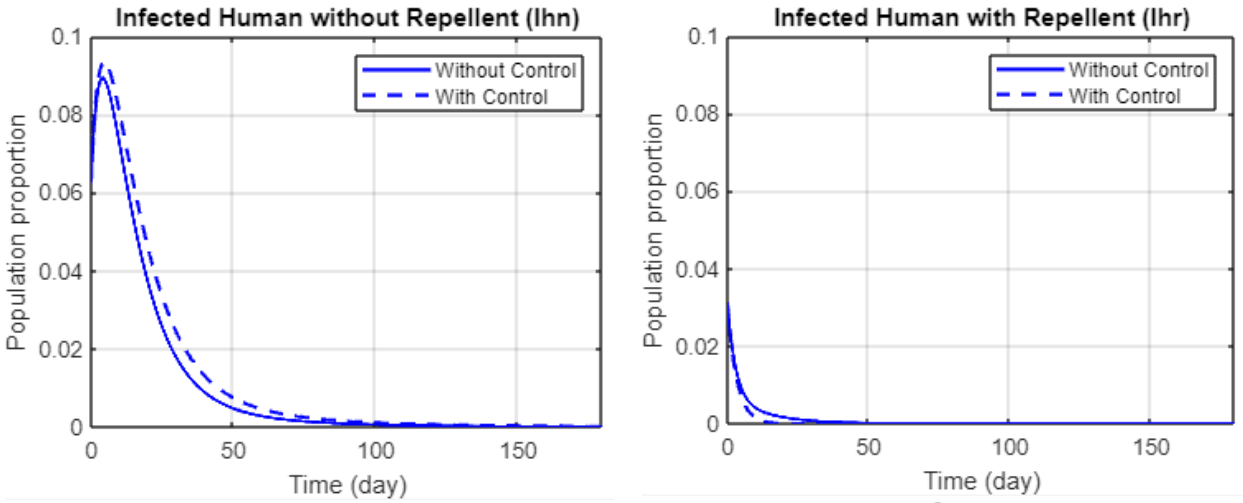

(a) **(b)**

Figure 9. Numerical Simulation Result of Controlling the Proportion Healthy Humans Who Have Impacted by Campaign and Used Repellent Regularly (a) Infected Human without Repellent, (b) Infected Human with Repellent

Figure 9 shows the dynamic of i and i_{hr} without and with control u_2. **Figure 9**(a) shows that i_{hn} with control increases to 0.389% at the peak of infection. After that, i_{hn} with control decreased slower by 0.647% than the i_{hn} without control. While **Figure 9**(b) shows that i_{hr} with control decreases to 0.255% compared to the i_{hr} without control. With the decreasing of i_{hr}, the control of campaign rate for using repellent in the early of infection period will reduce the potensial of virus transmission.

Figure 10 shows the dynamic of r_{hn} and r_{hr} without and with control u_2. From **Figure 10**(a), $r_{hn}$with control increases to 28.961% compared to the r_{hn} without control. While **Figure 10**(b) shows that r_{hr} with control decreases to 21.201% until the proportion limit to zero. The control of campaign rate implies the repellent used regularly (u_2) since early of infection period is more work effectively to minimize the infected population and maximize the recovered population.

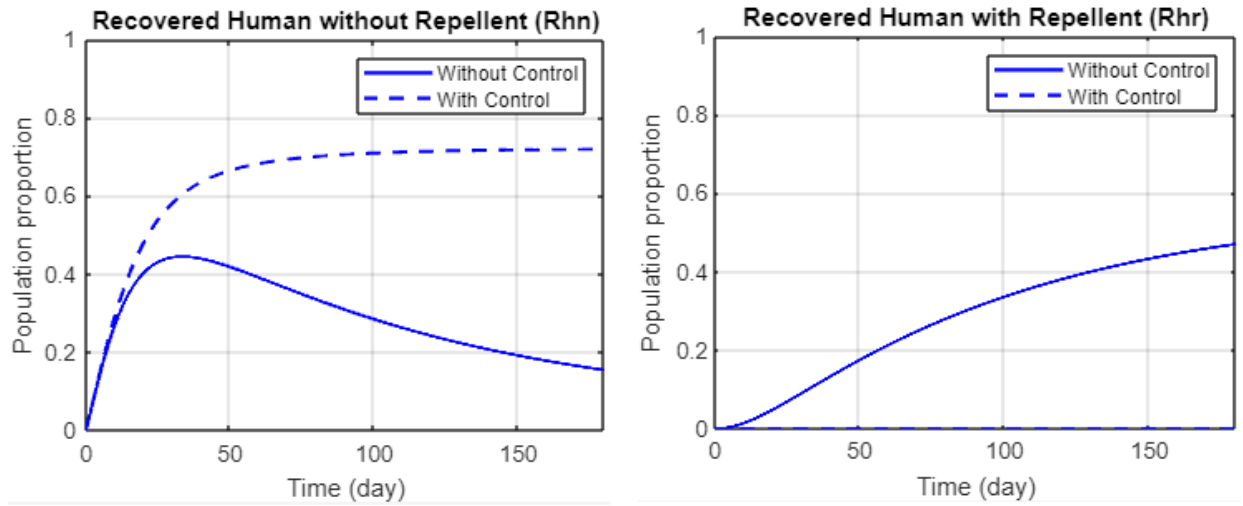

(a) **(b)**

Figure 10. Numerical Simulation Result of Controlling the Proportion of Healthy Humans Who Have Impacted by Campaign and Used Repellent Regularly (a) Recovered Human without Repellent, (b) Recovered Human with Repellent

Figure 11- Figure 13 shows the dynamic for a human population when the combination of control u_1 and control u_2 applied to the systems. Combination control is applied to compare which strategy can provide optimal effectiveness in reducing the infected human population for both prevention and treatment control scenarios. However, combination control will result in a larger cost function compared to implementing a single control u_1 and u_2 respectively.

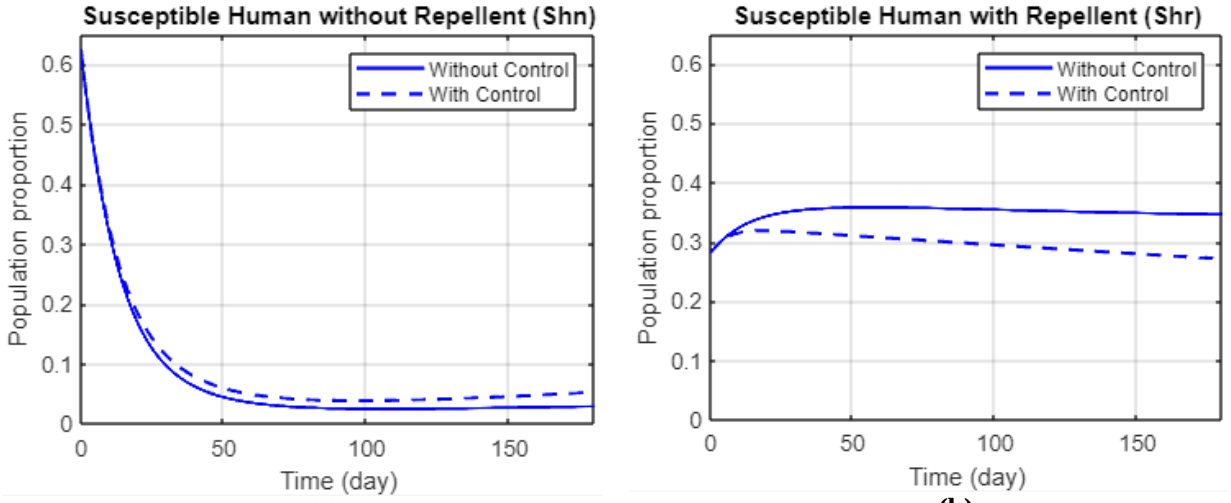

(a) **(b)**

Figure 11. Numerical Simulation Result of Controlling the Usage Rate of Repellent and the Proportion of Healthy Humans Who Have Impacted by Campaign and Used Repellent Regularly (a) Susceptible Human without Repellent, (b) Susceptible Human with Repellent

Figure 11 shows the dynamic of s_{hn} and s_{hr} without and with combination control (u_1, u_2). From **Figure 11**(a), s_{hn} with control increases slower by 1.434% than the s_{hn} without control. Meanwhile, **Figure 11**(b) shows that the combination control (u_1, u_2) causes the s_{hr} with control decreases quite large by 5.881% compared to the s_{hr} without control. Combination control (u_1, u_2) which applied to susceptible human population has the same dynamics with single control u_1 and u_2. The potential for transmission in healthy human populations will also tend to have a small chance. However, the effect of combination control (u_1, u_2) causes the smallest decreasing compared to single control u_1 and u_2.

Figure 12 shows the dynamic of i_{hn} and i_{hr} without and with combination control (u_1, u_2). From **Figure 12**(a), i_{hn} with control increases to 0.075% at the peak of infection. After that, i_{hn} decreases slower by 0.438% than the i_{hn} without controls. Meanwhile, **Figure 12**(b) shows that the combination control (u_1, u_2) cause the i_{hr} with control decreases to 0.131% compared to the i_{hr} without controls. **Figure 13** shows the dynamic of r_{hn} and r_{hr} without and with combination control (u_1, u_2). **Figure 13**(a) shows that r_{hn} with control increases to 23.611% compared to the r_{hn} without controls. While **Figure 13**(b) shows that the combination control (u_1, u_2) causes the r_{hr} with control decreases to 19.186%. Dynamic of infected and recovered population with combination control (u_1, u_2) has the almost same percentage effect with dynamic of infected and recovered population with single control u_1.

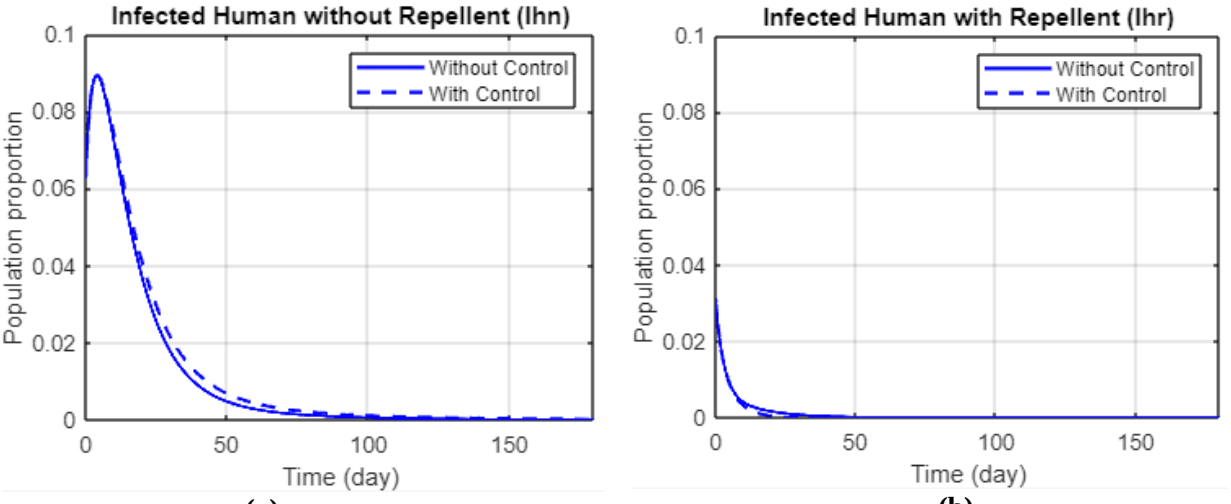

(a) **(b)**

Figure 12. Numerical Simulation Result of Controlling the Usage Rate of Repellent and the Proportion of Healthy Humans Who Have Impacted by Campaign and Used Repellent Regularly (a) Infected Human without Repellent, (b) Infected Human with Repellent

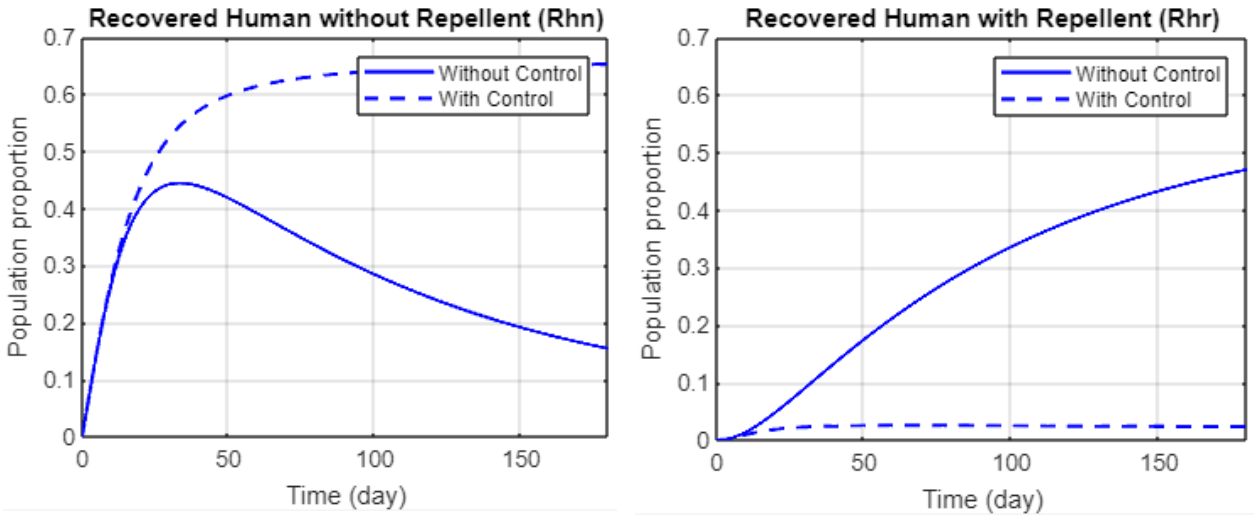

(a) **(b)**

Figure 13. Numerical Simulation Result of Controlling the Usage Rate of Repellent and the Proportion of Healthy Humans Who Have Impacted by Campaign and Used Repellent Regularly (a) Recovered Human without Repellent, (b) Recovered Human with Repellent

Table 3. Comparison of Objective Function Values for Three Strategies

Strategy	Objective Function Value
Controlling the Rate of Repellent Treatment $\boldsymbol{u_1}$	2.9936
Controlling the Proportion of Healthy Humans Who Have Impacted by Campaign and Used Repellent Regularly $\boldsymbol{u_2}$	2.2695
Combination Control $\boldsymbol{u_1}$ and $\boldsymbol{u_2}$	3.0808

Table 3 shows the accumulative objective function for each control strategy, both single control u_1 and u_2 and combination control (u_1, u_2). Based on the value of the objective function in Table 3, control u_1, i.e. the proportion of healthy humans who have been impacted by the campaign and used repellent regularly is the most effective strategy to suppress the spread of dengue fever with an accumulative cost is 2.2695.

4. CONCLUSIONS

Based on the analysis and numerical simulations, we can conclude the effect of parameters on the dengue fever spread model and the most effective strategy to suppress the spread of dengue fever. First, a higher transmission rate of dengue leads to a faster spread of the disease. Second, a faster recovery rate from the disease slows down its transmission. Third, increased human use of repellent results in a slower rate of dengue transmission. Fourth, a longer duration of repellent protection also contributes to a slower rate of dengue spread. Fifth, controlling the proportion of healthy people who have the campaign's effect and use repellent regularly is the most effective strategy to suppress the spread of dengue fever. This implies that using repellents with long-lasting protection can serve as a control strategy to reduce or manage the spread of dengue.

ACKNOWLEDGMENT

The authors would like to thanks the referees for their valuable comments and suggestions. Parts of the research are funded by the Community Service and Innovation Research Grant (PPMI) ITB 2023.

REFERENCES

[1] M. G. Guzman, D. J. Gubler, A. Izquierdo, E. Martinez and S. B. Halstead, "Dengue Infection," *Nature Review Disease Primer,* p. 16055, 2016.

[2] M. L. Moi, Y. Ami, C.-K. Lim, Y. Suzaki, Y. Saito, K. Kitaura, M. Saijo, R. Suzuki, I. Kurane and T. Takasaki, "Formation of infectious dengue virus-antibody immune complex in vivo in marmosets (Callithrix jacchus) after passive transfer of anti-dengue virus monoclonal antibodies and infection with dengue virus," *The American Journal of Tropical Medicine and Hygiene,* vol. 92, no. 2, pp. 370-376, 2015.

[3] V. H. Ferreira-de-Lima and T. N. Lima-Camara, "Natural vertical transmission of dengue virus in Aedes aegypti and Aedes albopictus: a systematic review," *Parasites & Vectors,* vol. 11, 2018.

[4] Central for Disease Control and Prevention, "Transmission," WHO, 2019. [Online]. Available: www.cdc.gov/dengue/transmission/index.html. [Accessed 15 September 2022].

[5] L. R. Bowman, S. Donegan and P. J. McCall, "Is Dengue Vector Control Deficient in Effectiveness or Evidence?: Systematic Review and Meta-analysis," *PLoS Negl Tropc Dis,* vol. 10, no. 3, 2016.

[6] World Healthy Organization, "Dengue and Severe Dengue," WHO, 2022. [Online]. Available: https://www.who.int/news-room/fact-sheets/detail/ dengue-and-severe-dengue. [Accessed 22 September 2022].

[7] Indonesian Health Ministry, "Entering the Season Transition, the Ministry of Health Asks the Health Office to Be Wary of a Surge in Dengue Fever," Indonesian Health Ministry, 2022. [Online]. Available: https://sehatnegeriku.kemkes.go.id/baca/umum/20220923/3741130/masuk-peralihan-musim-kemenkes-minta-dinkes-waspadai-lonjakan-dbd. [Accessed 29 September 2022].

[8] T. A. Prasetyo, R. Saragih and D. Handayani, "Optimal Control on the Mathematical Models of Dengue Epidemic by Giving Vaccination and Repellent Strategies," in *Journal of Physics: Conference Series*, 1490 012034, 2020.

[9] Central for Disease Control and Prevention, "Vaccine Safety and Effectiveness," WHO, 2023. [Online]. Available: https://www.cdc.gov/dengue/vaccine/parents/safety-effectiveness. [Accessed 4 August 2023].

[10] W. H. Organization, "General Risk Assesment Models for Insecticide-trated Clothing, Skin-Applied Repellents and Household Insecticides," WHO, 2019.

[11] J. W. Tang, W. P. Bahnfleth, P. M. Bluyssen, G. Buonanno, J. L. Jimenez, J. Kurnitski, Y. Li, S. Miller, C. Sekhar, R. Morawska, L. C. Marr, A. K. Melikov, W. Nazaroff, P. V. Nielsen, R. Tellier, P. Wargocki and S. J. Dancer, "Dismantling myths on the airborne transmission of severe acute respiratory syndrome coronavirus-2 (SARS-CoV-2)," *The Journal of Hospital Infection,* vol. 110, pp. 89-96, 2021.

[12] N. C. Achaiah, S. B. Subbarajasetty and R. M. Shetty, "R0 and Re of COVID-19: Can We Predict When the Pandemic Outbreak will be Contained?," *Indian Journal of Critical Care Medicine,* vol. 24, no. 11, p. 1125, 2020.

[13] G. O. Fosu, E. Akweittey and A. Adu-Sackey, "Next-Generation Matrices and Basic Reproductive Numbers for All Phases of The Coronavirus Disease," *Open Journal of Mathematical Sciences,* vol. 4, no. 1, pp. 261-272, 2020.

[14] N. A. Lestari, Sutimin, S. Khabibah, R. H. S. Utomo, R. Herdiana and A. H. Permatasari, "Local Stability Analysis for Tuberculosis Epidemic Model with Different Infection Stages and Treatments," in *Journal of Physics: Conference Series*, 1943 012120, 2020.

[15] F. Brauer, C. Castillo-Chavez and Z. Feng, "Endemic Disease Models," *Mathematical Models in Epidemiology,* vol. 69, pp. 63-116, 2019.